A Study of Subunit Interface Residues of Fructose-1,6-bisphosphatase by Site-Directed Mutagenesis: Effects on AMP and Mg^{2+} Affinities†

Lie-Fen Shyur, Alexander E. Aleshin, and Herbert J. Fromm*

Department of Biochemistry and Biophysics, Iowa State University, Ames, Iowa 50011

Received February 15, 1996; Revised Manuscript Received April 3, 1996⊗

ABSTRACT: The structural transformation of fructose-1,6-bisphosphatase upon binding of the allosteric regulator AMP dramatically changes the interactions across the C1−C4 (C2−C3) subunit interface of the enzyme. Asn9, Met18, and Ser87 residues were modified by site-directed mutagenesis to probe the function of the interface residues in porcine liver fructose-1,6-bisphosphatase. The wild-type and mutant forms of the enzyme were purified to homogeneity and characterized by initial rate kinetics and circular dichroism (CD) spectrometry. No discernible alterations in structure were observed among the wild-type and Asn9Asp, Met18Ile, Met18Arg, and Ser87Ala mutant forms of the enzyme as measured by CD spectrometry. Kinetic analyses revealed 1.6- and 1.8-fold increases in k_{cat} with Met18Arg and Asn9Asp, respectively. The K_m for fructose 1,6-bisphosphate increased about 2−∼4-fold relative to that of the wild-type enzyme in the four mutants. A 50-fold lower K_a value for Mg^{2+} compared with that of the wild-type enzyme was obtained for Met18Ile with no alteration of the K_i for AMP. However, the replacement of Met18 with Arg caused a dramatic decrease in AMP affinity (20 000-fold) without a change in Mg^{2+} affinity. Increases of 6- and 2-fold in the K_i values for AMP were found with Asn9Asp and Ser87Ala, respectively. There was no difference in the cooperativity for AMP inhibition between the wild-type and the mutant forms of fructose-1,6-bisphosphatase. This study demonstrates that the mutation of residues in the C1−C4 (C2−C3) interface of fructose-1,6-bisphosphatase can significantly affect the affinity for Mg^{2+}, which is presumably bound 30 Å away. Moreover, the mutations alternatively reduce AMP and Mg^{2+} affinities, and this finding may be associated with the destabilization of the corresponding allosteric states of the enzyme. The kinetics and structural modeling studies of the interface residues provide new insights into the conformational equilibrium of fructose-1,6-bisphosphatase.

Fructose-1,6-bisphosphatase (D-fructose-1,6-bisphosphate 1-phosphohydrolase, EC 3.1.3.11, FBPase),[1] a key regulatory enzyme in the gluconeogenesis pathway, is a homotetramer with a subunit molecular mass of approximately 37 kDa. It catalyzes the hydrolysis of fructose 1,6-bisphosphate (Fru-1,6-P_2) to fructose 6-phosphate (Fru-6-P) and inorganic phosphate (P_i). The catalytic activity requires divalent metal ions such as Mg^{2+}, Mn^{2+}, and Zn^{2+} (Benkovic & deMaine, 1982; Tejwani, 1983). FBPase is highly regulated, (*i.e.*, its activity is inhibited competitively by fructose 2,6-bisphosphate and noncompetitively by AMP), and the action of these two compounds is synergistic (Liu & Fromm, 1988; Pilkis *et al.*, 1988; Van Schaftingen & Hers, 1981). The hydrolysis of Fru-1,6-P_2 with FBPase is hyperbolic with inhibition at high substrate concentrations. The binding of Mg^{2+} to FBPase exhibits sigmoidal kinetics with a Hill coefficient of 2 at neutral pH, but is hyperbolic at pH 9.6 (Liu & Fromm, 1990; Nimmo & Tipton, 1975a). The AMP inhibition also shows cooperativity with a Hill coefficient of approximately 2 (Stone & Fromm, 1980; Nimmo & Tipton, 1975b; Taketa & Pogell, 1965). Unfortunately, it is still not clear how the cooperativity relative to Mg^{2+} and AMP occurs.

The solution of the crystal structure of FBPase has shown that each subunit of the enzyme consists of two domains, an allosteric AMP domain (residues 1−200) and an active site Fru-1,6-P_2 domain (residues 200−335) (Ke *et al.*, 1990). The AMP binding site in each subunit is about 30 Å from the active site, and the metal binding sites are located near the active site (Figure 1) (Xue *et al.*, 1994; Liang *et al.*, 1992; Ke *et al.*, 1989). Kinetic and binding studies have shown that AMP and Mg^{2+} are mutually exclusive in their binding to FBPase (Liu & Fromm, 1990; Scheffler & Fromm, 1986). The tightness of AMP binding is enhanced by Fru-2,6-P_2, which is attributed to a decrease in the k_{off} for the nucleotide (Liu & Fromm, 1988). Crystallographic studies have also shown that the binding of AMP to FBPase shifts some residues of the metal binding sites to positions unfavorable for the metal binding (Zhang *et al.*, 1994). Mutation of the amino acid residues in the metal binding site can affect the ligand affinity of metal ions and AMP (Chen *et al.*, 1993), and alternatively, the alteration of some of the amino acid residues in the AMP domain changes not only the AMP affinity but also the Mg^{2+} affinity (Shyur *et al.*, 1996).

The crystallographic investigations of pig kidney FBPase demonstrated that the conformation of the enzyme changes from the so-called R-state to the T-state upon binding of AMP (Zhang *et al.*, 1994; Villeret *et al.*, 1995; Ke *et al.*, 1991). The major feature of this structural transition is a 17° rotation of the C1−C2 dimer relative to the C3−C4 dimer and a 1.9° rotation of the AMP binding domain relative

† This research was supported in part by Research Grant NS 10546 from the National Institutes of Health, U. S. Public Health Service, and Grants MCB-9218763 and MCB-9316244 from the National Science Foundation. This is Journal Paper J-16739 of the Iowa Agriculture and Home Economics Experiment Station, Ames, IA; Project 3191.

* To whom correspondence should be addressed.

⊗ Abstract published in *Advance ACS Abstracts,* June 1, 1996.

[1] Abbreviations: FBPase, fructose-1,6-bisphosphatase; Fru-1,6-P_2, fructose 1,6-bisphosphate; Fru-6-P, fructose 6-phosphate; Fru-2,6-P_2, fructose 2,6-bisphosphate; CD, circular dichroism.

S0006-2960(96)00367-4 CCC: $12.00

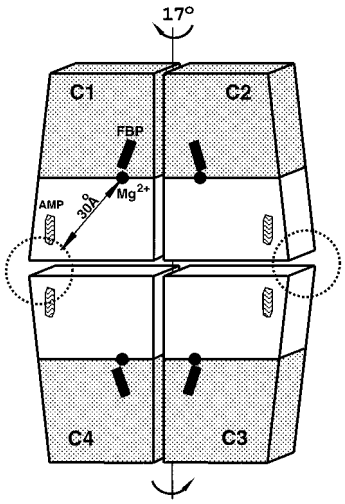

FIGURE 1: Schematic drawing of the FBPase tetramer in the R conformation. The subunits are labeled according to Zhang *et al.* (1994). The stippled halves of the subunits are Fru-1,6-P_2 domains, and the white halves are AMP domains. The approximate positions of the AMP, Fru-1,6-P_2 (FBP), and Mg^{2+} binding sites are shown. The dashed circles indicate the mutated area. The quaternary structure of the T-form differs by the rotation of the C1−C2 dimer relative to the C3−C4 dimer.

to the Fru-1,6-P_2 domain (Figure 1). The movement of the subunits dramatically changes the interactions between the AMP binding domains across C1−C4 and symmetrically related C2−C3 subunit interfaces. For example, Asn9 (C1) interacts with Asn83 (C4) in the R-state and with Ser87 (C4) in the T-state. A new hydrogen bond is observed between Ser87 (C1) and Arg15 (C4) in the T-state. The distance between the side chains of Met18 of C1 and C4 changes from 11.7 to 3.8 Å. In an attempt to probe the roles of Asn9, Met18, and Ser87 residues during the allosteric transition and to determine whether these residues are involved in the structural stabilization of the R- or the T-state of FBPase, we have prepared FBPase mutants at those positions by site-directed mutagenesis, and the kinetic properties of Asn9Asp, Met18Ile, Met18Arg, and Ser87Ala were studied. The most interesting finding of this study is that the replacement of Met18 by Ile causes significant changes in Mg^{2+} affinity, whereas the Met18Arg mutant exhibits a dramatic decrease in AMP affinity. These results, when compared with the kinetic properties of other interface mutants (Shyur *et al.*, 1996), indicate that all investigated mutations do not significantly influence the affinity for Mg^{2+} and AMP simultaneously; *i.e.*, a change in the AMP affinity without altering Mg^{2+} binding and *vice versa*.

EXPERIMENTAL PROCEDURES

Materials. Fru-1,6-P_2, Fru-2,6-P_2, NADP, $MgCl_2$, AMP, and IPTG were purchased from Sigma. DNA-modifying and restriction enzymes were from Promega and Clontech Laboratories, Inc. Glucose-6-phosphate dehydrogenase and phosphoglucose isomerase were obtained from Boehringer Mannheim. Other chemicals were of reagent grade or the equivalent.

Mutagenesis of FBPase. Mutations were accomplished by the introduction of specific base changes into a double-stranded plasmid (Deng & Nickoloff, 1992). Four mutagenic primers, as shown in Table 1, were used to mutate Asn9→Asp, Met18→Ile, Met18→Arg, and Ser87→Ala. A selective primer, which exchanged the original *Nru*I site for a unique *Xho*I site on the pET-11a vector, and the sequencing primers are also shown in Table 1. The double-stranded FBPase expression plasmid (pET-FBP) (Burton *et al.*, 1993) and mutagenic and selective primers were denatured, annealed, and polymerized as described by Deng and Nickoloff (1992).

Table 1: Oligonucleotide Primers Used in Site-Directed Mutagenesis

mutants	mutagenic primer[a] sequences
Asn9Asp	5′-CTTCGACACC**G**ATATCGTCAC-3′
Met18Ile	5′-GCTTCGTCAT**A**GAGGAGGGC-3′
Met18Arg	5′-CGCTTCGTCA**G**GGAGGAGGG-3′
Ser87Ala	5′-GTGTTAAAG**G**CATCTTTT-3′
selective primer:	5′-CAGCCTCGCCTCGAGAACGCCA-3′
sequencing primers:	5′-GAATTGTGAGCGGATAAC-3′ [b]
	5′-CACAAGGCAGTCGATGTT-3′ [c]

[a] Boldface and underlined letters indicate mismatches. [b] The sequencing primer was used for confirming the mutations of Asn9Asp, Met18Ile, and Met18Arg mutants. [c] The sequencing primer was used for confirming the mutations of the Ser87Ala mutant.

Mutations were confirmed by *Nru*I/*Xho*I digestion and by fluorescent dideoxy chain-termination sequencing at the Nucleic Acid Facility at Iowa State University. The mutagenesis plasmid was finally transformed into *Escherichia coli* DF 657, a strain deficient in the FBPase gene.

Purification of Wild-Type and Mutant FBPase. The wild-type and Asn9Asp, Met18Ile, Met18Arg, and Ser87Ala FBPases were purified by using 30−70% $(NH_4)_2SO_4$ precipitation, a Sephadex G-100 column, and a CM-Sephadex C-50 column. The experimental details are described elsewhere (Burton *et al.*, 1993; Shyur *et al.*, 1995).

Protein concentration was assayed as described by Bradford (1976) with bovine serum albumin (from Sigma) as the standard. The protein purity was determined by using 12% SDS−polyacrylamide gel electrophoresis according to Laemmli (1970).

Kinetic Studies. Specific activity during purification was determined by the phosphoglucoisomerase and glucose-6-phosphate dehydrogenase coupled spectrometric assay at pH 7.5 and pH 9.6 (Liu & Fromm, 1990; Ulm *et al.*, 1975). All other kinetic experiments were done at pH 7.5 (Hepes buffer) and 24 °C by using a coupled spectrofluorometric assay (Liu & Fromm, 1990). Initial rate data were analyzed by using a computer program written in MINITAB language with an α value of 2.0 (Liu & Fromm, 1990; Siano *et al.*, 1975). Cooperativity was evaluated by using either the ENZFITTER program (Leatherbarrow, 1987) or the MINITAB program.

Circular Dichroism Spectrometry. CD studies on the wild-type and mutant forms of FBPase were carried out in a Jasco J710 CD spectrometer in a 1 mm cell at room temperature. Spectra were collected from 200 to 260 nm in 1.3 nm increments, and each spectrum was blank-corrected and smoothed by using the software package provided with the instrument.

Model Building. The structural models for Met18Ile and Met18Arg mutants of FBPase were built from the X-ray structures of the R- and T-states of the wild-type enzyme (Zhang *et al.*, 1993; Xue *et al.*, 1994) using the program QUANTA (Molecular Simulation Inc.). The best conformations of the side chains of Ile and Arg at the position of Met18 were obtained by conformational search and then energy-minimized. The coordinates of all residues except

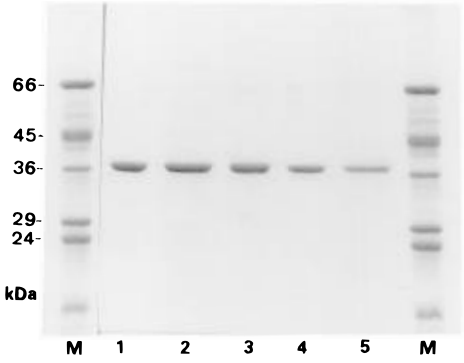

FIGURE 2: SDS−polyacrylamide gel electrophoresis of purified wild-type and mutant forms of porcine liver fructose-1,6-bisphosphatase. A 12% SDS minigel was used and stained with Coomassie Brilliant Blue R-250. M: Molecular mass standards. Lane 1, wild-type. Lanes 2−5, Asn9Asp, Met18Ile, Met18Arg, and Ser87Ala mutants, respectively.

those in the 8 Å zone around the mutated residue were fixed at their crystallographic positions.

RESULTS

Purification of the Wild-Type and Mutant Forms of FBPase. The enzyme purity of the wild-type and four mutant forms of porcine liver FBPase was evaluated by SDS−PAGE. Figure 2 shows, by using electrophoresis as a criterion, that these enzymes exhibit identical mobilities and are greater than 96% homogeneous. These same similarities were found in the wild-type and mutants during column chromatography and, in addition, in the yield of pure enzyme as determined from the protein concentrations when assayed by the Bradford method (1976). The yield of pure enzyme is about 1−2 mg/g of cells. The pH 7.5/pH 9.6 activity ratios shown in Table 2, along with the SDS−PAGE results suggest that the enzymes had not undergone proteolysis (Ulm *et al.*, 1975).

Secondary Structure Analysis. CD spectrometry was used to analyze the secondary structure of the mutant FBPases and the wild-type enzyme. The CD spectra of the five enzymes are superimposable from 200 to 260 nm (data not shown). These results indicated that no major conformational changes occurred in the mutant FBPases based on the use of CD as a criterion of the secondary structure of the proteins.

Kinetic Properties of FBPase Mutants. To evaluate the effects of mutations on residues at the C1−C4 and C2−C3 interfaces of FBPase, initial rate kinetic studies were undertaken with the wild-type and mutant forms of the enzyme. The kinetic parameters are summarized in Table 2. The data were obtained at a concentration of Fru-1,6-P_2 or Mg^{2+} that does not cause substrate inhibition. A 1.6- and 1.8-fold increase in k_{cat} compared with that of wild-type enzyme was found with mutants Met18Arg and Asn9Asp, respectively, suggesting that the catalytic efficiencies are enhanced in both mutants. Small increases (2-fold) in Fru-1,6-P_2 affinity were observed in Met18Ile, Met18Arg, and Ser87Ala, and a 4-fold increase was found in Asn9Asp relative to wild-type FBPase.

Mg^{2+} Ion Activation. The activity of wild-type FBPase, as a function of Mg^{2+} concentration, was sigmoidal at neutral pH with a Hill coefficient of approximately 2 (Nimmo & Tipton, 1975a; Tashima & Yoshimura, 1975). In this study, the Hill coefficient for Mg^{2+} and the K_a for Mg^{2+} of the wild-type and mutant forms of FBPase were determined at their saturating Fru-1,6-P_2 concentrations (12−20 μM). The effect of Mg^{2+} concentration was shown to be sigmoidal with a Hill coefficient of approximately 2 for the four mutants as well as in the case of the wild-type enzyme (Table 2). However, different K_a values for Mg^{2+} were observed when mutations were made at the residues at the subunit interface of FBPase. A significant increase in K_a for Mg^{2+} (∼50-fold) was observed for Met18Ile, but only small changes (1.5−∼1.8-fold) were found in Asn9Asp, Met18Arg, and Ser87Ala. Various alterations of Mg^{2+} affinity were also reported for the mutants of helix H1 residues of FBPase, *e.g.*, 9-fold for Arg15Ala and 5-fold for Glu19Gln, and no changes for Arg22Lys and Arg22Met(Shyur *et al.*, 1996). The large change in Mg^{2+} affinity for Met18Ile is somewhat surprising because it indicates that the influence of the mutation can be effectively transferred 30 Å away to the metal binding sites.

Fru-2,6-P_2 Inhibition. Fru-2,6-P_2 is a competitive inhibitor of FBPase ligated with residues located at the active site. Table 2 shows that the K_i value for Fru-2,6-P_2 was decreased 5-fold for Met18Ile compared with the wild-type enzyme, and only small changes were found for Asn9Asp, Met18Arg, and Ser87Ala. The increased inhibition of Met18Ile mutant by Fru-2,6-P_2 correlates with reduced affinity for Mg^{2+}. Moreover, Table 3 shows that the correlation of altered affinity for Mg^{2+} and Fru-2,6-P_2 was also observed in other interface mutants, *i.e.*, Arg15Ala and Glu19Gln. The K_m values of Fru-1,6-P_2 for these mutants were also decreased slightly. These results suggest that the three residues located at the interface of subunits are not important in permitting FBPase to discriminate between the substrate and inhibitor. In other words, the three residues do not play a significant role in Fru-2,6-P_2 inhibition of FBPase.

Kinetics of AMP Inhibition. AMP is an allosteric regulator of FBPase (Stone & Fromm, 1980; Nimmo & Tipton, 1975b; Taketa & Pogell, 1965). The action of AMP inhibition is nonlinear noncompetitive with respect to Fru-1,6-P_2, but nonlinear competitive relative to Mg^{2+} for wild-type FBPase (Liu & Fromm, 1990). The binding of AMP with FBPase shows cooperativity with a Hill coefficient of approximately 2.0 (Stone & Fromm, 1980; Nimmo & Tipton, 1975b; Taketa & Pogell, 1965). Figure 3 shows a double-reciprocal plot of 1/velocity versus $1/[Mg^{2+}]^2$ in the presence and absence of AMP for Met18Arg FBPase. The data in Figure 3 gave excellent fits to eq 1, which is consistent with a steady-state random mechanism, when $n = 2$. The form of eq 1 is

$$\frac{1}{v} = \frac{1}{V_m}\left[1 + \frac{K_a}{A^2}\left(1 + \frac{I}{K_i} + \frac{I^n}{K_{ii}} + \frac{I}{K_{iii}} + \frac{I^n}{K_{iv}}\right) + \frac{K_b}{B} + \frac{K_{ia}K_b}{A^2B}\left(1 + \frac{I}{K_i} + \frac{I^n}{K_{ii}}\right)\right] \quad (1)$$

where v, V_m, A, B, I, K_a, K_b, K_{ia}, K_i, K_{ii}, K_{iii}, and K_{iv} represent the initial velocity, the maximal velocity, the concentrations of Mg^{2+}, Fru-1,6-P_2, and AMP, respectively, the Michaelis constants for Mg^{2+} and Fru-1,6-P_2, the dissociation constants for Mg^{2+}, and the dissociation constants for AMP from the enzyme−AMP, enzyme−AMP−AMP, enzyme−Fru-1,6-P_2−AMP, and enzyme−Fru-1,6-P_2−AMP−AMP complexes, respectively. n represents the Hill coefficient for AMP with FBPase. When $n = 2$, the binding of AMP to

Table 2: Kinetic Parameters for Wild-Type and Mutant Forms of Fructose-1,6-bisphosphatase

enzyme	specific activity	pH 7.5/9.5	k_{cat} (s^{-1})	K_m(Fru-1,6-P_2) (μM)	K_i(Fru-2,6-P_2) (μM)	K_i[a](AMP) (μM)	K_a(Mg^{2+}) (mM^2)	Hill coefficient (Mg^{2+})
wild-type	30.9 ± 2.80	3.0	18.0 ± 1.70	3.51 ± 0.24	0.24 ± 0.02	20.5 ± 5.72	0.49 ± 0.22	1.97 ± 0.12
Asn9Asp	52.3 ± 3.79	3.1	31.9 ± 2.31	0.90 ± 0.07	0.17 ± 0.01	127 ± 8.98	0.87 ± 0.06	2.19 ± 0.11
Met18Ile	33.9 ± 2.17	2.0	20.6 ± 1.31	1.68 ± 0.13	0.05 ± 0.00	22.4 ± 0.07	24.3 ± 2.90	1.88 ± 0.09
Met18Arg	46.7 ± 2.45	2.4	28.3 ± 1.49	1.76 ± 0.10	0.37 ± 0.02	0.51 ± 0.08[b]	0.74 ± 0.08	1.84 ± 0.12
Ser87Ala	33.7 ± 1.82	2.4	20.5 ± 1.11	1.91 ± 0.13	0.18 ± 0.01	43.1 ± 4.96	0.85 ± 0.07	2.10 ± 0.13

[a] The K_i was obtained from plots of 1/velocity versus 1/[Fru-1,6-P_2] at 5 mM Mg^{2+}. [b] The K_i for the Met18Arg mutant FBPase is in mM^2.

Table 3: Kinetic Properties of FBPase Mutants Relative to Those of Wild-Type Enzyme[a]

enzyme	k_{cat}	K_m(Fru-1,6-P_2)	K_i(Fru-2,6-P_2)	K_i(AMP)	K_a(Mg^{2+})	preferred state[b]
Asn9Asp	~2/1	1/4	1	6/1	~2/1	R
Met18Arg	~2/1	1/2	1	25000/1	1	R
Arg22Met	2/1	1	1/2	1	1/~2	R(?)[c]
Arg15Ala	1	1	1/6	1/~3	9/1	T
Met18Ile	1	1/2	1/5	1	50/1	T
Glu19Gln	1	1/3	1/5	1	5/1	T
Arg22Lys	1	1/2	2/1	30/1	1	?
Thr27Ala	1	1/4	2/1	1350/1	2/1	?
Ser87Ala	1	1/~2	1	2/1	~2/1	?

[a] The kinetic properties are shown by the ratio of mutant/wild-type FBPase of kinetic data from Table 2 in this paper and Table 2 reported by Shyur *et al.* (1996). [b] The preferred state of the mutants in the absence of AMP. [c] ? mean same as wild-type enzyme.

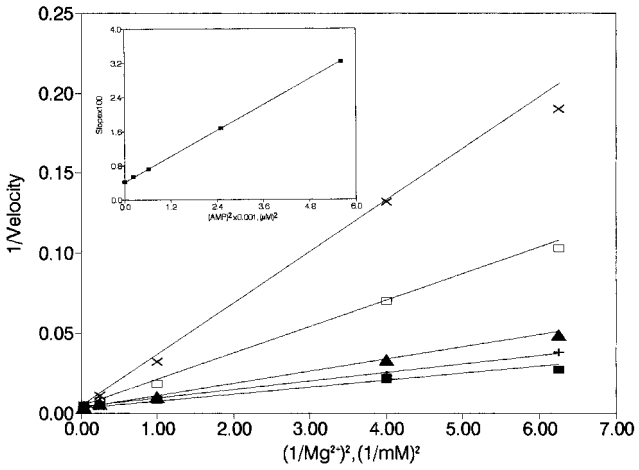

FIGURE 3: Plot of reciprocal of initial velocity in arbitrary fluorescent units *versus* reciprocal of $[Mg^{2+}]^2$ for Met18Arg FBPase. The concentrations of AMP are 0 (■), 15 μM (+), 25 μM (▲), 50 μM (□), and 75 μM (×). The coupled spectrofluorescence assay was performed at 25 °C in 50 mM Hepes buffer (pH 7.5) containing 0.1 M KCl, 10 μM Fru-1,6-P_2. The lines are theoretical based upon eq 1 when $n = 2$, and the points were experimentally determined. The inset shows a plot of the slope of the family of curves in Figure 1 *versus* $[AMP]^2$.

FBPase exhibits cooperativity; on the other hand, there is no cooperativity when $n = 1$. The kinetic data from experiments similar to those shown in Figure 3 for wild-type, Met18Ile, Asn9Asp, and Ser87Ala mutant FBPases fit best to eq 1 when $n = 2$ (data not shown). The "Goodness of Fit" was <6% when $n = 2$ in all cases. The results indicate that AMP cooperativity is not altered with these mutants. On the basis of eq 1, I is a competitive inhibitor for substrate A (Mg^{2+}) and will be a noncompetitive inhibitor for substrate B (Fru-1,6-P_2) in the reaction. When the Fru-1,6-P_2 concentration was varied at different fixed concentrations of AMP, a family of lines intersecting to the left of the 1/velocity axis was obtained for the double-reciprocal plots (data not shown). These data were best fit to eq 1 when $n = 2$. The K_i value obtained from the experiment shows a greater than 20 000-fold decrease in AMP affinity relative to wild-type FBPase observed with the Met18→Arg mutation. Interestingly, no change in the K_i for AMP in Met18Ile FBPase and only a 2- and a 6-fold increase in K_i for AMP for Ser87Ala and Asn9Asp were observed. These results show that these residues contribute different effects to AMP affinity without disrupting the cooperativity for inhibitor binding.

DISCUSSION

Lipscomb and co-workers, on the basis of their crystallographic studies of pig kidney FBPase, proposed a mechanism for the allosteric regulation of the enzyme (Zhang *et al.*, 1994; Villeret *et al.*, 1995; Ke *et al.*, 1991). According to their model, FBPase exists in two conformational states stabilized by different sets of hydrogen bonds across C1−C4 and symmetry-related C2−C3 subunit interfaces. These interfaces are formed by the residues of the AMP domains of the enzyme, so it was interpreted that binding AMP initiates the transition from the active R-state to the inactive T-state. Though X-ray analysis of FBPase identified the potential sets of the interactions involved in the stabilization of each state, it did not provide information concerning the role of each interface residue in the mechanism of the transition and about the requirement of AMP for the transition to occur. It is obvious that the energy of AMP binding stabilizes the T-state, but are the free energies of the enzyme in the R- and the T-states so different that the transition cannot occur in the absence of AMP?

Here, we report kinetic studies on the mutants of the three interface residues Asn9, Met18, and Ser87 of porcine liver FBPase, whose deduced amino acid sequence is identical to that of kidney FBPase (Burton *et al.*, 1993; William & Kantrowitz, 1992). Of the three residues investigated, the most interesting one is Met18, which, contrary to the current view concerning the importance of hydrogen bonds in the stabilization of the allosteric states of FBPase, is not involved in intersubunit hydrogen bond interactions. The mutation of Met18 to Ile and Arg caused significant and opposite effects: the first mutation reduced the Mg^{2+} affinity, and

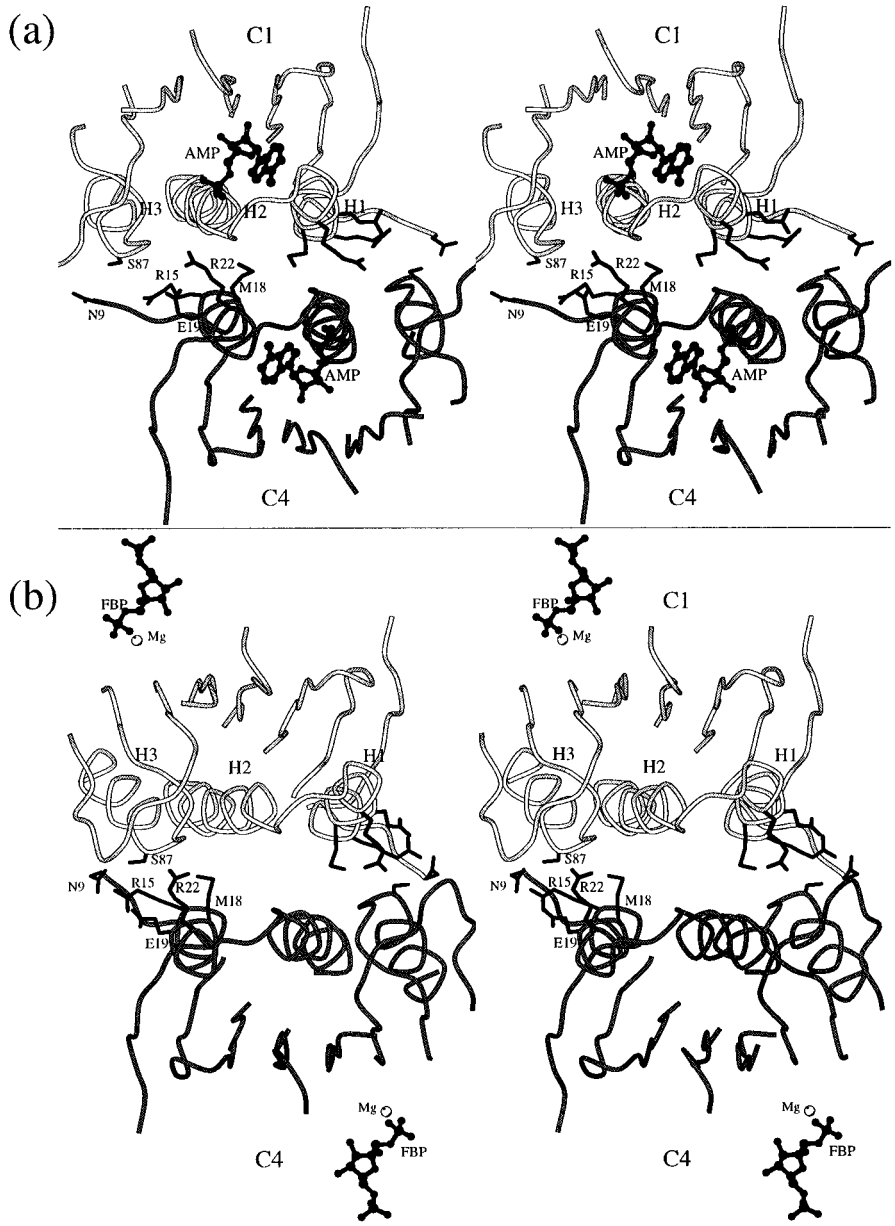

FIGURE 4: Stereo drawing of the C1−C4 subunit interface of FBPase in the T-state (a) and in the R-state (b). The view is along the axis of molecular symmetry between the C1 subunit (open coil) and the C4 subunit (filled coil). The side chains of mutated residues (Table 3) as well as bound AMP, Fru-1,6-P_2, and Mg^{2+} are shown. The figure was prepared by MOLSCRIPT (Kraulis, 1991) using the coordinates from the Protein Data Bank (entries FBC and FRP).

the second reduced the AMP affinity. That Mg^{2+} affinity may be influenced by the alteration of the C1−C4 (C2−C3) interface residues was observed earlier (Shyur *et al.*, 1996); however, the currently reported change of the Mg^{2+} affinity is so significant that it cannot be dismissed as some sort of side effect and thus requires an explanation within the model of the allosteric regulation.

The influence of interface mutations on the AMP and Mg^{2+} affinities can be interpreted by either one of the following mechanisms: (1) a local disturbance of the conformation of a subunit, which affects the corresponding binding site; or (2) as a shift of the equilibrium of the two states toward the one in which the ligand is bound more weakly (in the second case, the deformation of the binding sites is not necessary). In a previous paper (Shyur *et al.*, 1996), we were able to successfully explain the changes in the AMP affinities of Thr27Ala and Arg22Lys mutants within the first mechanism. Lu *et al.* (1995) suggested that both mechanisms seem likely in the case of the Arg22Ala mutant of FBPase; however, that mutation resulted in an alteration of AMP affinity. However, in the case of the reduced Mg^{2+} affinity observed with the Met18Ile mutant, explaining the direct influence of the mutation at the Mg^{2+} site is somewhat tenuous because of the remoteness of the Mg^{2+} binding site relative to the site of mutation (Figures 1 and 4). A comparison of kinetic properties of Arg15Ala, Met18Ile, and Glu19Gln (Table 3) demonstrates that reduction of Mg^{2+} affinity in these mutants occurs without a change in AMP inhibition. Within the first model, this would mean that the distortions from the mutated residues of Glu19Gln, Arg15Ala, and especially Met18Ile can be effectively transferred through the AMP domain to the Mg^{2+} binding site and, at the same time, do not disturb the AMP binding site. This would be possible if there was very sensitive communication between the C1−C4 (C2−C3) interface and the metal binding sites.

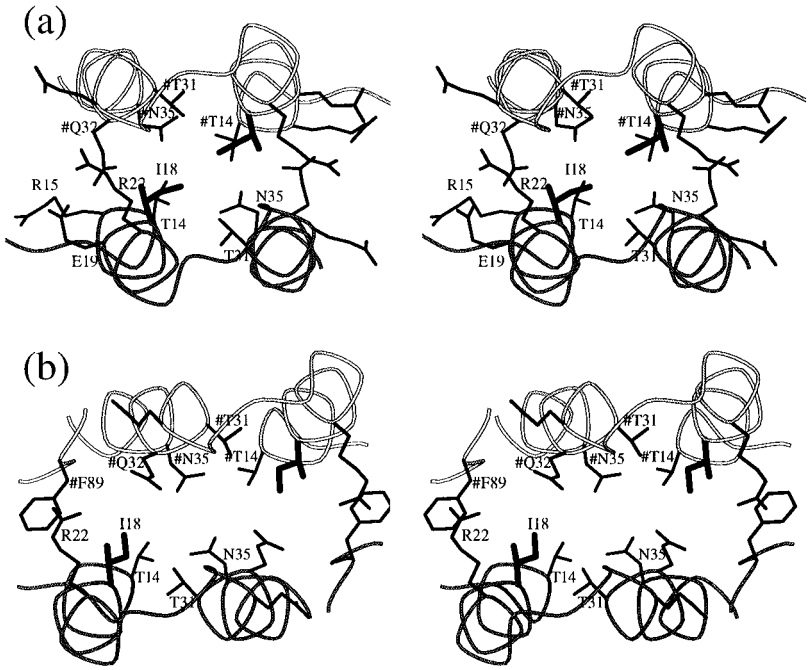

FIGURE 5: Stereoviews of the enlarged region around Ile18 in the modeled Met18Ile mutant of FBPase from Figure 4: (a) in the T conformation; (b) in the R conformation. The side chains of all residues in the 5 Å area around Ile18 are shown.

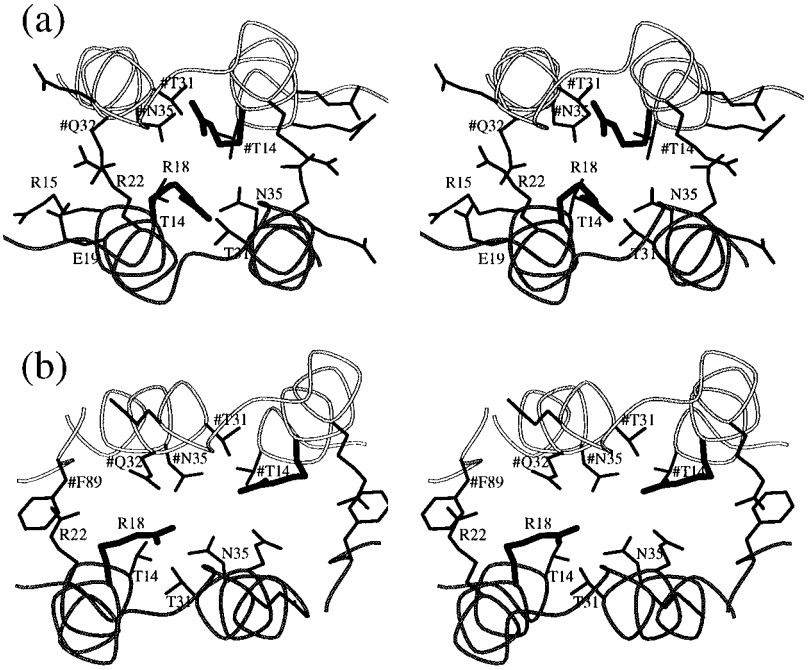

FIGURE 6: Stereoviews of the region around Arg18 in the modeled Met18Arg mutant of FBPase: (a) in the T conformation; (b) in the R conformation. The views are identical to those in Figure 5.

The alternative mechanism for the reduction of AMP and Mg^{2+} affinities due to the shift of the equilibrium of the T- and the R-states explains the effect of the interface mutations on Mg^{2+} binding without distortion of the subunits. It, however, requires that the enzyme be able to transit into the T-state in the absence of AMP and that the Mg^{2+} affinity is different in the R- and the T-states. This suggestion is consistent with the observation that AMP and Mg^{2+} antagonistically influence the enzyme activity, *i.e.*, AMP inhibits and Mg^{2+} activates. This result can be interpreted as a predominant binding of AMP and Mg^{2+} in the T- and the R-states, respectively.

The structural analysis of the Met18Ile and Met18Arg mutants based on the X-ray structures of wild-type FBPase (Zhang *et al.*, 1993; Xue *et al.*, 1994) favors the hypothesis of the shifted state equilibrium and weakens the subunit distortion hypothesis in the case of the Met18Ile mutant. The Ile18 side chain with staggered dihedral angles fits nicely into both R- and T-state interfaces (Figure 5). Substitution of methionine with isoleucine is electrostatically neutral, and neither the side chain of Met18 nor that of Ile is involved in hydrogen bond interactions. Taking into account that less conservative mutations of neighboring residues such as Glu19Gln and Arg15Ala produced weaker effects on Mg^{2+}

affinity, it is rather unlikely that the substitution of Met18 with Ile could disturb the Mg^{2+} binding site, which is positioned 30 Å away (Figure 1 and Figure 4). On the other hand, this mutation can influence the equilibrium of the allosteric states. A comparison of the crystal structures of the R- and T-states of FBPase demonstrates that the C1−C4 subunit interface is more open in the R-state than in the T-state (Figure 4). The water-accessible area of the Met18 side chain (and that of its Ile substitute) is twice as large in the R-state as in the T-state (20 $Å^2$ *vs* 10 $Å^2$). Thus, the polar methionine stabilizes the R-state more favorably than the T-state. In addition, the sulfur atoms of the symmetric Met18s in the T-state are in direct van der Waals contact with each other in what obviously causes their electrostatic repulsion. The substitution of Met18 with the more hydrophobic isoleucine removes unfavorable electrostatic interactions of the T-state and increases the relative free energy of the R-state because of the more hydrophilic environment of Ile18. Thus, the Met18Ile substitution presumably shifts the initial equilibrium of the R- and T-states toward the T-state. If the assumption concerning the differential binding of Mg^{2+} in the allosteric states of FBPase is correct, then the relative destabilization of the R-state can explain the reduced Mg^{2+} affinity.

The mutation of Met18→Arg produces an effect opposite to that of the Met18Ile mutant of FBPase. The modeling demonstrates that the Arg side chain fits more poorly than that of Met, and thus, Arg is able to influence the conformation of FBPase subunits in both R- and T-states more dramatically, although the substitution does not change the affinity for Mg^{2+}. A comparison of the structural models of the Met18Arg mutant in the R- and T-states suggests that the substitution significantly destabilizes the T-state relative to the R-state. In the T-state, the symmetrically related Arg18s are 8 Å closer to each other than in the R-state, and their guanidinium groups are in direct contact and therefore electrostatically repulse each other (Figure 6). A better charge separation plus a more hydrophilic environment of arginines serves to stabilize the R-state. Thus, like the Met18Ile mutant, the effect of Met18Arg substitution on AMP affinity can be reasonably explained by the relative destabilization of one state over the other. Moreover, it is quite possible that the mutation affects the ligand binding site because the main chain of the mutated residue is involved in the formation of the AMP binding site. Thus, it is likely that, in all interface mutations affecting AMP affinity, both mechanisms operate simultaneously.

The mutated Asp9 and Ser87 residues belong to the same area of the C1−C4 (C2−C3) interface as Met18, but their alteration produces weaker effects on AMP and Mg^{2+} affinities. Ser87 presumably is involved in intersubunit hydrogen bonding with symmetrically related Asn9 in the T-state of the enzyme and with Glu19 in the R-state. That the Ser87Ala mutant exhibits kinetic properties similar to those of the wild-type enzyme suggests that the hydrogen bond interactions involving Ser87 are not important for the transition between the R- and T-states. The mutation of Asn9 to Asp, however, influences AMP affinity (Table 2). The effect produced by this mutation correlates with those produced by Arg15Ala, Met18Ile, Met18Arg, and Glu19Gln, the mutants of the residues from the same area of the interface (Figure 4). Table 3 demonstrates that the mutation of charged Arg15 and Glu19 to electrostatically neutral Ala15 and Gln19, as well as polar Met18 to hydrophobic Ile, reduces the Mg^{2+} affinity but does not disturb AMP binding. On the other hand, the substitution of electrostatically neutral Asn9 and Met18 by charged Asp9 and Arg18 reduces AMP affinity. If AMP and Mg^{2+} affinities in these mutants change due to the destabilization of one state over the other, then the observed correlation suggests that the charged residues in this area of the interface are important for the formation of the R-state.

REFERENCES

Benkovic, S. T., & deMaine, M. M. (1982) *Adv. Enzymol. Relat. Areas Mol. Biol. 53*, 45−82.

Bradford, M. M. (1976) *Anal. Biochem. 72*, 248−254.

Burton, V. A., Chen, M., Ong, W.-C., Ling, T., Fromm, H. J., & Stayton, M. M. (1993) *Biochem. Biophys. Res. Commun. 192*, 511−517.

Chen, L., Hegde, R., Chen, M., & Fromm, H. J. (1993) *Arch. Biochem. Biophys. 307*, 350−354.

Deng, W. P., & Nickoloff, J. A. (1992) *Anal. Biochem. 200*, 81−88.

Ke, H., Thorpe, C. M., Seaton, B. A., & Lipscomb, W. N. (1989) *J. Mol. Biol. 212*, 513−539.

Ke, H., Zhang, Y., & Lipscomb, W. N. (1990) *Proc. Natl. Acad. Sci. U.S.A. 87*, 5243−5247.

Ke, H., Liang, J.-Y., Zhang, Y., & Lipscomb, W. N. (1991) *Biochemistry 30*, 4412−4420.

Kraulis, P. J. (1991) *J. Appl. Crystallogr. 24*, 946−950.

Laemmli, U. K. (1970) *Nature 227*, 680−685.

Leatherbarrow, R. J.(1987) ENZFITTER: A Non-linear Regression Data Analysis Program for the IBMPC, pp 13−75, Elsevier Science Publishers BV, Cambridge/United Kingdom.

Liang, J.-Y., Huang, S., Zhang, Y., Ke, H., & Lipscomb, W. N. (1992) *Proc. Natl. Acad. Sci. U.S.A. 89*, 2404−2408.

Liu, F., & Fromm, H. J. (1988) *J. Biol. Chem. 263*, 9122−9128.

Liu, F., & Fromm, H. J. (1990) *J. Biol. Chem. 265*, 7401−7406.

Lu, G., Williams, M. K., Giroux, E. L., & Kantrowitz, E. R. (1995) *Biochemistry 34*, 13272−13277.

Nimmo, H. G., & Tipton, K. F. (1975a) *Eur. J. Biochem. 58*, 567−574.

Nimmo, H. G., & Tipton, K. F. (1975b) *Eur. J. Biochem. 58*, 575−585.

Pilkis, S. J., El-Maghrabi, M. R., & Claus, T. H. (1988) *Annu. Rev. Biochem. 57*, 755−783.

Scheffler, J. E., & Fromm, H. J. (1986) *Biochemistry 25*, 6659−6665.

Shyur, L. F., Zhang, R., & Fromm, H. J. (1995) *Arch. Biochem. Biophys. 319*, 123−127.

Shyur, L. F., Aleshin, A. E., Honzatko, R. B., & Fromm, H. J. (1996) *J. Biol. Chem. 271*, 3005−3010.

Siano, D. B., Zyskind, J. W., & Fromm, H. J. (1975) *Arch. Biochem. Biophys. 170*, 587−600.

Stone, S. R., & Fromm, H. J. (1980) *Biochemistry 19*, 620−625.

Taketa, K., & Pogell, B. M. (1965) *J. Biol. Chem. 240*, 651−662.

Tashima, Y., & Yoshimura, N. (1975) *J. Biochem. 78*, 1161−1169.

Tejwani, G. A. (1983) *Adv. Enzymol. Relat. Areas Mol. Biol. 54*, 121−194.

Ulm, E. H., Pogell, B. M., deMaine, M. M., Libby, C. B., & Benkovic, S. J. (1975) *Methods Enzymol. 42*, 369−374.

Van Schaftingen, E., & Hers, H.-G. (1981) *Proc. Natl. Acad. Sci. U.S.A. 78*, 2861−2863.

Villeret, V., Huang, S., Zhang, Y., & Lipscomb, W. N. (1995) *Biochemistry 34*, 4307−4315.

William, M. K., & Kantrowitz, E. R. (1992) *Proc. Natl. Acad. Sci. U.S.A. 89*, 3080−3082.

Xue, Y., Huang, S., Liang, J.-Y., Zhang, Y., & Lipscomb, W. N. (1994) *Proc. Natl. Acad. Sci. U.S.A. 91*, 12482−12486.

Zhang, Y., Liang, J.-Y., Huang, S., Ke, H., & Lipscomb, W. N. (1993) *Biochemistry 32*, 1844−1857.

Zhang, Y., Liang, J.-Y., Huang, S., & Lipscomb, W. N. (1994) *J. Mol. Biol. 244*, 609−624.

BI960367+